Filtration of a Hanford Site Tank 241-AN-102 Waste Sample with Alternate Sr/TRU Precipitation Conditions at Bench and Pilot Scales

John R. Zamecnik
Michael R. Poirier
Mark R. Duignan
Charles A. Nash
Mark A. Baich

Westinghouse Savannah River Company

March 22, 2004

Filtration of a Hanford Site Tank 241-AN-102 Waste Sample with Alternate Sr/TRU Precipitation Conditions at Bench and Pilot Scales

John R. Zamecnik
Michael R. Poirier
Mark R. Duignan
Charles A. Nash
Mark A. Baich

Westinghouse Savannah River Company

Summary

In support of the design of the Hanford Waste Treatment Plant, the Savannah River Technology Center has conducted crossflow ultrafiltration tests on the bench scale with both a radioactive sample and simulants and at pilot scale with simulants. The waste tested was from Tank 241-AN-102, which underwent isotopic dilution with strontium nitrate to reduce the soluble ^{90}Sr concentration, and sodium permanganate precipitation to remove selected transuranic species. Experimental work validated the use of a simulant by comparison of bench scale simulant filtration data with radioactive filtration test data data. Tests on a pilot scale were also conducted and showed that the filtration flux in the pilot unit was consistently lower than in the bench scale unit. An alternative precipitation method resulted in less filterable slurries.

Several possible explanations for the differences in flux were proposed, including differences in particle size distribution and slurry viscosity (the term viscosity will be used, although consistency is more correct for non-Newtonian fluids). The experimental data was also fit to an empirical model and several filtration models. The trends in the data generally followed the predictions of the filtration models. Differences in flux between the bench and pilot scales could not be accounted for by the calculated difference in the average wall shear stress.

Introduction

The Savannah River Technology Center (SRTC) has conducted crossflow ultrafiltration tests to support the design of the Hanford Waste Treatment Plant (WTP). These filtration tests have been performed in three phases: bench-scale tests with actual radioactive waste (hot cells unit filter, or hot CUF) (Nash 2000a; Nash 2000b; Nash 2001), bench-scale tests with waste simulants (cold CUF) (Zamecnik 2003), and pilot-scale tests (Duignan 2003) with simulants. The waste tested was from Tank 241-AN-102, which is an “Envelope C” waste that contains significant amounts of organic chelating agents. In the WTP, Envelope C wastes will undergo isotopic dilution with strontium nitrate to reduce the soluble ^{90}Sr concentration, and sodium permanganate precipitation to remove selected transuranic (TRU) species. These two treatments are referred to as “Sr/TRU precipitation”. The goal of the filtration in the WTP is to increase the undissolved solids content of the precipitate slurry to at least 15 wt%.

The main goals of this experimental work were to validate the use of a simulant by comparing radioactive waste filtration test data with cold simulant waste bench-scale filtration data and then simulant waste bench-scale data with pilot-scale data. An alternative Sr/TRU precipitation method was also examined along with the baseline method at a lower temperature and the baseline method was evaluated with pulse jet mixing in place of mechanical agitation.

Simulant and Sr/TRU Precipitation

A simulant formulation developed by SRTC was used for this work (Eibling 2002). This simulant included both a supernate fraction and a solids fraction. The solids fraction of the simulant comprised only 0.1 weight percent of the total mass. Two slightly different simulant formulations were actually tested. Based on new information, the simulant used in the initial studies (called R1) was modified to contain more carbonate and less hydroxide for later studies (called R2). This change made the simulant composition match the real waste composition more accurately.

The precipitation process was done before the filtration of either the radioactive or cold simulated wastes. The Sr/TRU precipitation was performed by the following steps: dilution to 6.0M total sodium, addition of NaOH to a total hydroxide concentration of 1.0-1.2M, addition of $Sr(NO_3)_2$ at 50°C to give a final Sr concentration of 0.075M, and addition of $NaMnO_4$ at 50°C to give an added Mn concentration of 0.05M. This protocol is the “baseline” method that was used in both the radioactive and simulant tests. An alternate precipitation method (referred to as “alternate”) also tested removed the addition of NaOH, changed the final Sr and Mn concentrations both to 0.03M, and reduced the temperature to 25°C; this method was only tested with simulants. The precipitates generated gave slurries with ~1.5 wt% undissolved solids. A typical composition of the simulant is shown in Table 1.

Table 1 Typical R2 Simulant Liquid Fraction Composition

Species	mg/L	Species	mg/L	Species	mg/L
Al	9500	W	137	NO_2^-	54500
B	38.3	Zn	4.4	NO_3^-	137000
Ba	0.45	Zr	8.10	Cl^-	3700
Ca	407	K	2860	F^-	921
Cd	36.2	La	24.3	PO_4^{-3}	1970
Ce	28.8	Mg	1.0	SO_4^{-2}	10400
Co	1.4	Mn	16.6	formate	7350
Cr	156	Mo	30.7	oxalate	343
Cu	7.2	Na	137000	carbonate	27700
Fe	30.6	Nd	40.3	free OH- (M)	0.216
S	3380	Ni	265	total base (M)	1.66
Sr	2.9	P	696	specific gravity	1.32
Si	40.2	Pb	63.4	total solids (wt%)	34

A schematic of the cold CUF is shown in Figure 1. The multi-tube pilot system is similar to the single-tube CUF unit, but is on an engineering scale. Both systems consist of an agitated slurry reservoir, a pump, and a filter unit. Differences between these systems are shown in Table 2.

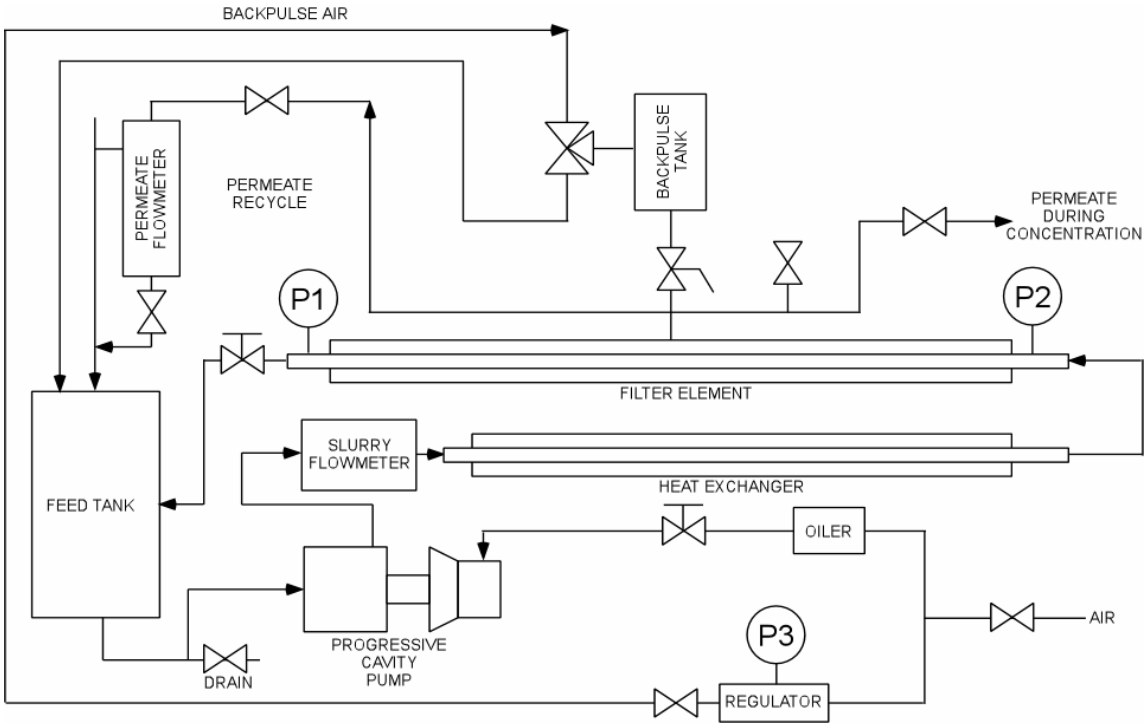

Figure 1 Cold CUF Filter System

Table 2 Comparison of CUF and Pilot Filtration Systems

Attribute	Units	Pilot	Cold CUF	Hot CUF
Tube Inside Diameter	inches	0.500	0.375	0.375
Number of Tubes		7	1	1
Tube Length	ft	7.5	2	2
Tube Inside Surface Area	ft^2	6.7	0.196	0.196
Pump Type		dual centrifugal	progressive cavity	progressive cavity
Data Collection		data acquisition system	manual	manual
Slurry Working Volume	L	~100	<6	<1

Test Conditions

Prior to each filtration test, the filters were cleaned by soaking in 2M HNO_3, followed by flushing with 0.01M NaOH. The fluxes of the NaOH solution (clean water) and also of a 5 wt% strontium carbonate slurry were measured both before and after each test. The clean water fluxes were not repeatable and varied greatly with the small amount of solids remaining in the filter system. Fluxes of the HNO_3 cleaning solution were much higher and more repeatable. The NaOH fluxes were much lower due to precipitation of small amounts of solids that were dissolved in the residual nitric acid in the system. The fluxes of the $SrCO_3$ test slurry were repeatable, but it was difficult to clean all of the slurry from the system without repeated flushing with large quantities of 0.01M NaOH.

The filtration conditions that were controlled in each test were the crossflow velocity (axial velocity in the tube) and the transmembrane pressure (TMP) which is the average pressure drop across the filter membrane. All filtration fluxes were determined by measuring the permeate flowrate; these fluxes were corrected to 25°C by the following formula:

$$F_{25} = F_T e^{2500\left(\frac{1}{273+T}-\frac{1}{298}\right)}$$

where F_{25} = corrected flux
F_T = flux at temperature T
T = temperature (°C)

Most of the hot CUF tests were conducted at 12 ft/s velocity and 50 psi TMP; others were conducted at 11 ft/s and 40 psi. Simulant tests were run at both of these conditions. The test conditions used are summarized in Table 3.

Table 3 Nominal Filtration Conditions

Test	Hot CUF	Cold CUF	Cold CUF	Pilot	Cold CUF	Pilot
Simulant	NA	R1	R2	R2	R2	R2
Sr/TRU Precipitation Conditions	Baseline	Baseline	Baseline	Baseline	Alternative	Alternative
Mean Axial Velocity (ft/s)	12 (11)	12	12	12	12	11.5
Mean TMP (psi)	50 (40)	50	40	40	40	42

The first cold CUF tests were done with the R1 simulant precipitate slurry that was made in nine small batches. With the first batch of precipitate slurry at ~1.5 wt% undissolved solids (UDS), the effects of transmembrane pressure and axial velocity were tested in a factorial arrangement. The precipitate slurry was then concentrated as each batch was fed over successive days and concentrated additionally to the final solids loading of about 19.3 wt%

undissolved solids. This test with the R1 simulant in small batches was not done in the pilot unit.

Because this concentration was higher than planned, the precipitate slurry was diluted with permeate back to 17.2 wt%. After an additional factorial arrangement of tests on the concentrated slurry was conducted, the slurry was then washed with an equal volume of 0.01M NaOH to reduce the soluble species concentrations. It was then re-concentrated to 20.6 wt% undissolved solids. Tests with the R1 simulant were not done in the pilot unit.

Both the baseline and alternate precipitation methods with the new simulant formulation (R2) were used to produce large batches of precipitate slurry that were tested in both the cold CUF and the pilot unit. For the R2 baseline tests, the cold CUF and pilot slurries were concentrated to 16.8 and 21.0 wt% UDS, respectively. The CUF precipitate slurry was concentrated to 14.8 wt% and the pilot precipitate slurry to 8.5 wt% in the alternate precipitation tests. Additional tests in the pilot unit were done with the baseline precipitation reaction conducted at 25°C rather than 50°C and also using pulse jet mixers instead of a standard agitator.

Filtration Models

Several filtration models were examined to determine if they could adequately describe the data. Note that none of the models examined accounted for the Bingham plastic behavior of the concentrated slurries.

Concentration Polarization Model

The concentration polarization model (Porter 1972) can be used to describe the dependence of the filtration flux on the wall shear stress, or velocity, in the tube. The form of this model will be used later to describe the dependence of the filtration flux on experimental variables. The general form of this model is given by Equation 1.

$$J = k \ln\left(\frac{C_W}{C_B}\right) \qquad \text{Equation 1}$$

where k = mass transfer coefficient
C_W = volumetric concentration at wall
C_B = volumetric concentration in bulk fluid

For laminar flow, the Graetz solution for convective heat transfer, modified for mass transfer, is:

$$\mathrm{Sh} = 1.62\left(\mathrm{ReSc}\frac{D}{L}\right)^{1/3} \qquad \text{Equation 2}$$

where Sh = Sherwood number = $\frac{kD}{\alpha D}$ $\quad$ ν = kinematic viscosity of slurry = $\frac{\mu}{\rho}$

Sc = Schmidt number $\frac{\nu}{D}$ $\quad$ μ = viscosity of slurry

ρ = density of slurry

Re = Reynolds Number = $\frac{DV}{\nu}$ $\quad$ D = tube diameter

V = velocity $\quad$ c = concentration

and $100 < \mathrm{ReSc}\frac{D}{L} < 5000$

Combining Equation 1 and Equation 2 gives Equation 3 for the flux in laminar flow.

$$J = 1.62\left(\frac{VD^2}{DL}\right)^{1/3} \ln\left(\frac{C_W}{C_B}\right) \text{ or } J \propto V^{1/3} \qquad \text{Equation 3}$$

In this model, the flux dependence on velocity is to the 1/3 power. A dependence on the tube diameter and tube length to the -1/3 power is also predicted.

For turbulent flow, the Dittus-Boelter relation rewritten for mass transfer may be used to describe the mass transfer coefficient as shown in Equation 4.

$$Sh = 0.023\ \mathrm{Re}^{0.8}\ \mathrm{Sc}^{1/3} \qquad \text{Equation 4}$$

Solving equation 4 for mass transfer coefficient yields $k = 0.023\frac{D^{2/3}V^{0.8}}{D^{0.2}\nu^{0.467}}$.

Solving for filter flux produces

$$J = 0.023\frac{D^{2/3}V^{0.8}}{D^{0.2}\nu^{0.467}}\left(\ln\frac{C_W}{C_B}\right) \quad or \quad J \propto V^{0.8}\mu^{-0.467} \qquad \text{Equation 5}$$

for Re>10000. This equation predicts that the flux should be dependent on the velocity to the 0.8 power and the slurry viscosity to the -0.467 power.

Model of Datta and Gaddis

Starting with the Kozeny-Carman drag relationship, Equation 6 and Equation 7 (Datta 1997) can be derived, which describe the permeate flow as a function of axial distance into the filter tube.

$$(R_m d^2 + r d^3)\frac{t_W}{\mu_c} = \frac{2\Delta P f}{\mu_P}\frac{C_B}{C_W - C_B}x \qquad \text{Equation 6}$$

$$r = \frac{9K\mu_0 C_W^2}{R^2(1-C_W)^3} \qquad \text{Equation 7}$$

where R_m = membrane hydraulic resistivity
r = cake hydraulic resistivity
d = cake thickness
t_W = wall shear stress
m_c = cake apparent viscosity
ΔP = transmembrane pressure
m_P = permeate viscosity
x = axial distance in tube
C_W = cake volume fraction solids
C_B = bulk fluid volume fraction solids
R = particle radius
K = Kozeny-Carman constant

The flux is generally described by:

$$J = \frac{\Delta P}{m_0 \left(R_m + rd \right)} \qquad \text{Equation 8}$$

and the dependence of the shear stress on velocity for turbulent flow can be derived from the friction factor and the Blasius equation:

$$t_W = \tfrac{1}{2} r V^2 f \quad \text{and} \quad f = 0.079 \mathrm{Re}^{0.25}$$

$$\text{gives } t_W = 0.0395 \left(\frac{n}{D} \right)^{0.25} V^{1.75} \qquad \text{Equation 9}$$

where f = friction factor

If the filter membrane resistivity is much less than the cake resistivity ($R_m << rd$), then Equation 6 - Equation 9 can be reduced to:

$$J = a\, m_P^{-4/3} m_C^{-1/3} V^{0.583} \left[\frac{C_W - C_B}{C_B} \frac{\left(1 - C_W\right)^6}{C_W^4} \right]^{1/3} \quad \text{or} \quad J \propto m_P^{-4/3} m_C^{-1/3} V^{0.583} \qquad \text{Equation 10}$$

where a = constant incorporating R, x, r, D, ΔP, and K

Equation 10 predicts that the flux will depend on the permeate viscosity to the -1.33, slurry viscosity to the -1/3, and velocity to the 0.583 power.

Effects of Transmembrane Pressure, Velocity, and Time

The factorial experiment flux measurements for the R1 baseline precipitation test were done to determine the functional dependence of the flux on the TMP (P) and axial velocity (V). For each set of test conditions of P,T, the flux versus time showed the typical exponential decay since each test condition was started with a backpulse. The steady-state fluxes for each test condition were then fit to give this model:

$$J = 0.0132 P^{0.0864} V^{0.627} t^{-0.122} \qquad \text{Equation 11}$$

where J = steady state flux (gpm/ft^2)
P = transmembrane pressure (psi, lb/in^2)
V = velocity (ft/s)
t = elapsed filtration time since start of test (hr)

The effect of pressure was marginally statistically insignificant at a 95% confidence, so it was left in the model. This model predicts that the maximum flux is achieved at the highest velocity

and pressure and the lowest elapsed time. The data fit to a model without the pressure term was:

$$J = 0.0199V^{0.590}t^{-0.123}$$ Equation 12

which is not significantly different.

The time factor accounts for the flux decrease seen due to the decrease in the particle size with time (duplicate tests performed at later times resulted in lower fluxes than the same tests run earlier). The particle size distributions of samples from several of the runs were measured using a Microtrac Particle Size Analyzer. Figure 2 and Figure 3 show the volume particle size distributions for the initial slurries and the concentrated slurries, respectively. In both figures, the legend lists the data from highest filtration flux to lowest flux. The alternate precipitation method tests had the lowest fluxes. The volume distribution prior to filtration shows no correlation with the flux, but the volume distribution after concentrating does correlate. The slurries with more particles in the 2-3 μm range filtered better relative to those with more particles in the 6-11 μm range. This observation means that the slurries with the smaller average particle size filtered better than those with larger particles, which is the opposite of what was expected. The population particle size distributions varied unpredictably and showed no correlation with flux.

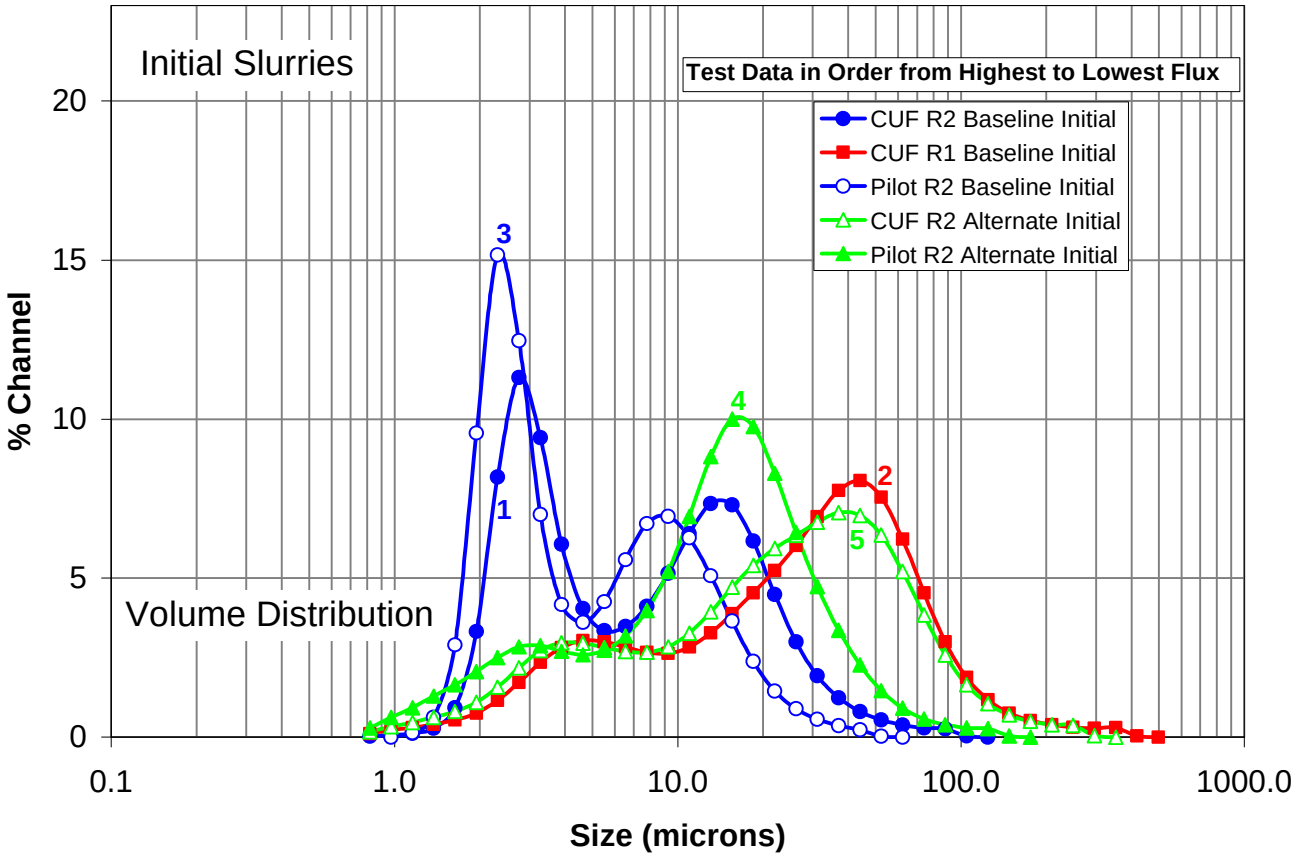

Figure 2 Volume Particle Size Distribution of Initial Slurries

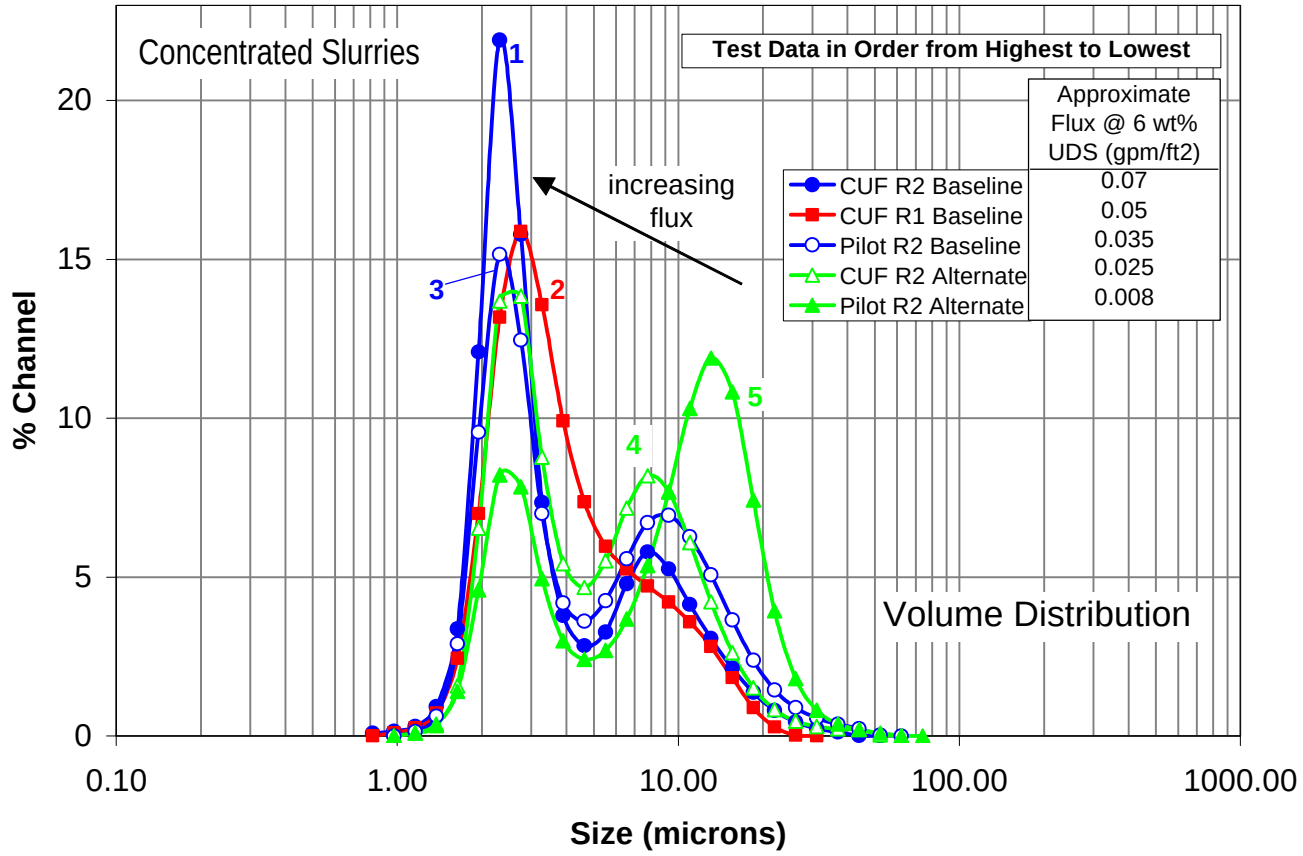

Figure 3 Volume Particle Size Distributions of Concentrated Slurries

The flux at 17.2 wt% insoluble solids was also fit to the same form of model, but with the time dependence fixed at the low insoluble solids slurry value ($t^{-0.122}$), as shown in Equation 2. At 17.2 wt%, the dependence of the flux on the TMP was not significant, and regression gave Equation 13.

$$J = 0.00894V^{0.627}t^{-0.122}$$ Equation 13

The empirical velocity dependence is compared to the three models in Table 4. The empirical model's velocity dependence agrees with the Datta & Gaddis model the best.

Table 4 Comparison of Velocity Dependence

Model	Power on Velocity
Empirical	0.627
Concentration Polarization – Laminar	0.333
Concentration Polarization – Turbulent	0.8
Datta & Gaddis – Turbulent	0.583

Filtration Flux as a Function of Slurry Solids Concentration

The flux data obtained during the concentration of the R1 precipitate slurry from 1.5 to 19.3 wt% were fit to the form of the concentration polarization model described by Equation 14.

$$J = 0.0283 \ln\left(\frac{8.22}{C_B}\right) \qquad \text{Equation 14}$$

where C_B was the measured bulk concentration. The mass transfer coefficient and the wall concentration were both fit as parameters. The wall concentration in wt% is 26.8, which is a reasonable value compared to measurements of filter cake solids concentrations.

There was no dependence on velocity since the concentration of the precipitate slurry was performed at a constant TMP and velocity of 50 psi and 12 ft/s, respectively. A plot of the data and the curve fit are shown in Figure 4. Figure 4 also shows the fit of the flux of washed slurry, which is described below.

Effect of Permeate Viscosity on Filtration Flux

The R1 precipitate slurry at 17.2 wt% insoluble solids was washed with an equal volume of 0.01 M NaOH and then re-concentrated to an undissolved solids value of 20.6 wt%. This washing step reduces the amount of soluble species that go to High Level Waste, while increasing the amount to Low Activity Waste. Soluble components washed out were Al, Na, nitrate, nitrite, chloride, fluoride, phosphate, sulfate, and formate.

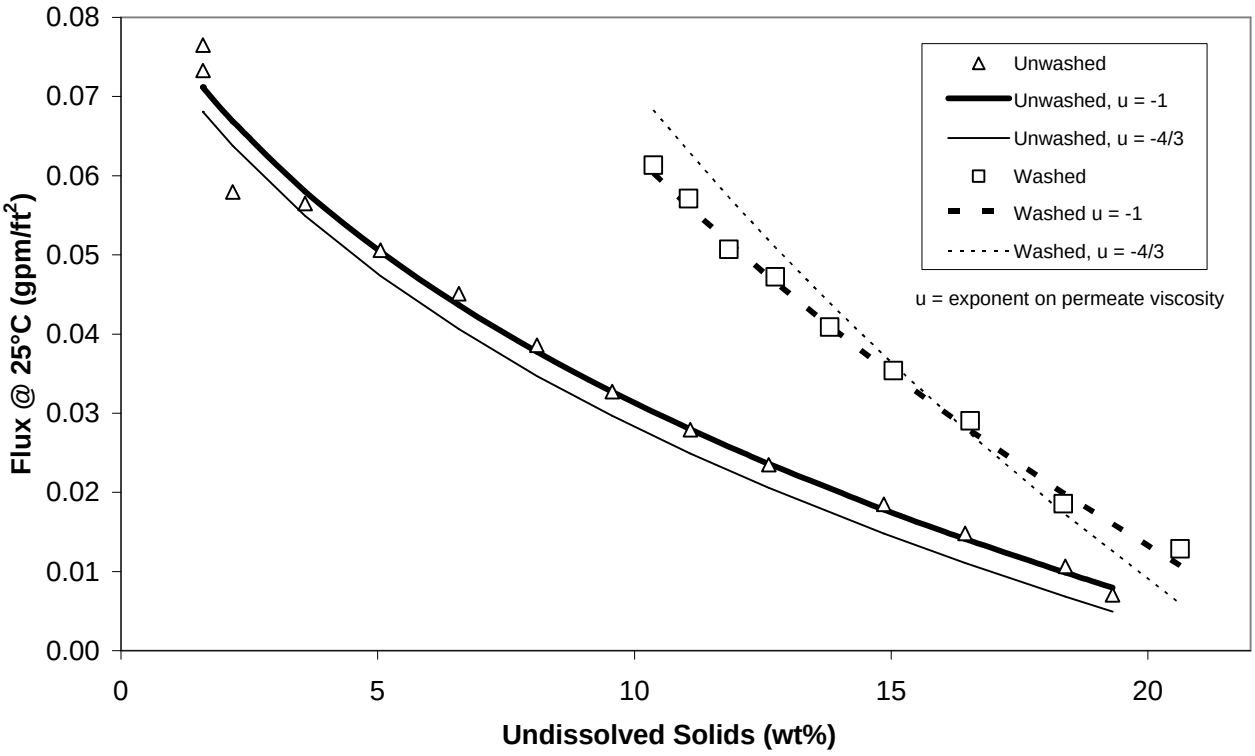

Figure 4 Predicted Flux versus Undissolved Solids

The effect of the permeate viscosity was accounted for by adding an inverse viscosity term:

$$J = 0.0877 m_P^{-1} \ln\left(\frac{8.22}{C_B}\right) \quad \text{Equation 15}$$

where $m_P =$ permeate viscosity (mPa•s)

This viscosity correction is based on the modified Hagen-Poiseuille equation (Porter 1990) shown in Equation 16 The flux through a porous medium is a function of the inverse of the viscosity. Of the variables in Equation 16, only the permeate viscosity differed between the unwashed and washed slurry.

$$J = \frac{d^2 e \Delta P}{32 m_P L} \quad \text{or} \quad J \propto m_P^{-1} \quad \text{Equation 16}$$

where J = flux
d = average pore diameter
e = bed porosity
DP = transmembrane pressure
m_P = permeate viscosity
L = pore length

Equation 10 predicts the permeate viscosity dependence to be to the -4/3 power. The fit of the data with this dependence, shown in Figure 4, is not as good as the -1 power dependence.

Filtration Flux Differences Between Tests

Figure 5 shows the flux versus undissolved solids content for radioactive, R1 simulant baseline, and R2 simulant baseline concentration tests. The R1 simulant and the radioactive test data agree very well, but the R2 concentration data are higher, especially at the beginning. Also shown is a single set of R2 data for a test where the precipitate slurry was not concentrated. The initial flux for this data set is also higher. Factors that could have affected the flux were examined to determine what caused the R2 fluxes to be higher. Note that the precipitation conditions for all of these tests were the same baseline conditions.

Differences between how the batches were processed were:

- The R1 simulant had less carbonate, which reacts with $Sr(NO_3)_2$ in the precipitation reaction to form $SrCO_3$.
- The R1 and radioactive tests used multiple small batches of precipitate slurry vs. the R2 concentration used one large batch.
- The R1 and radioactive tests started with 10-20 hours of factorial experiment testing prior to starting concentrating vs. no delay for the R2 concentration test.
- The R1 and radioactive tests were performed over nine or more days vs. the R2 concentration being performed over two days.
- The “cleanliness” of the filter prior to each test may have been different.

The carbonate content may have had an effect, but the R2 simulant matches the radioactive sample carbonate concentration better, so this difference would not seem to account for the observed differences. The factorial experiments in the R1 and radioactive tests resulted in declines of the flux in time at the same process conditions, indicating that particle degradation made the slurry harder to filter. This effect is also seen in the R2 single point data, where the same conditions were run for several hours and the flux declined by about 0.04 gpm/ft^2.

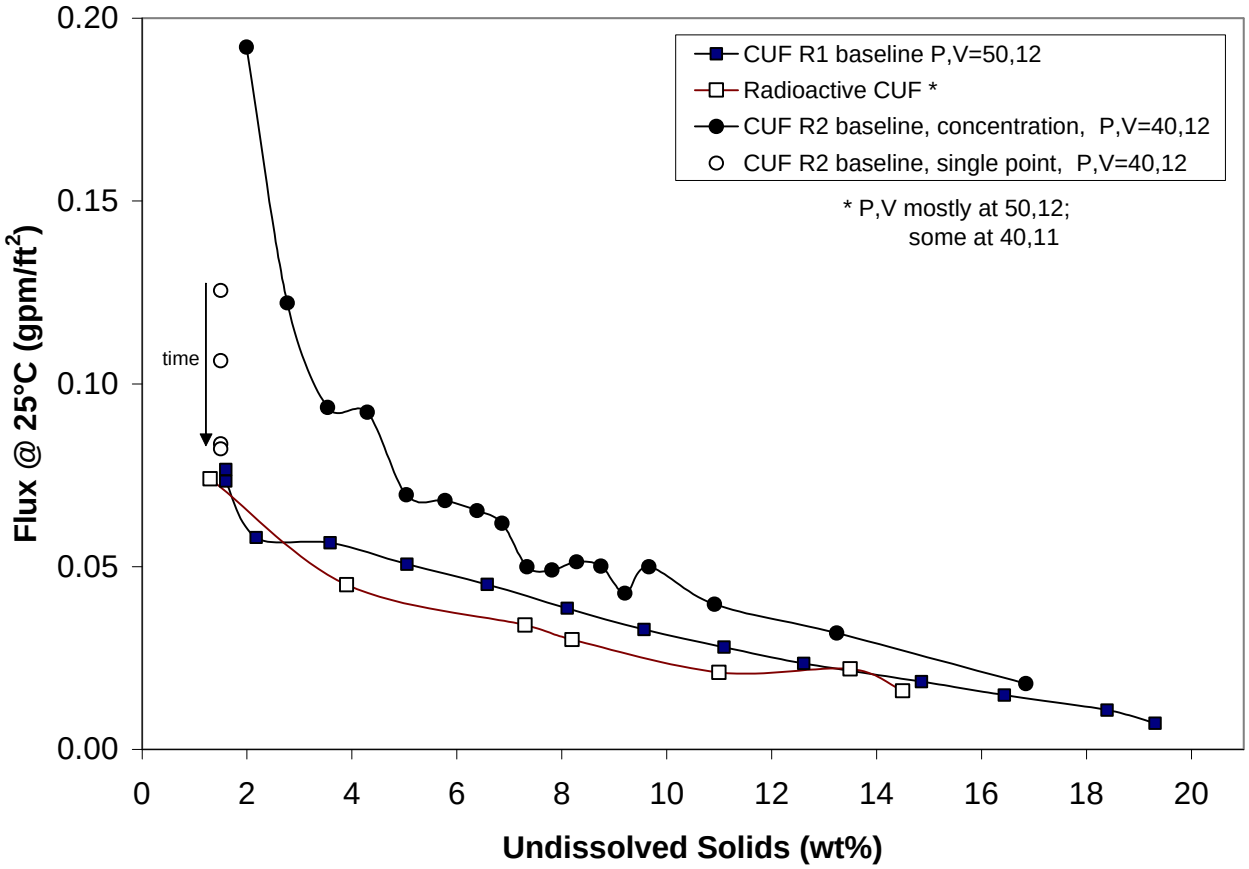

Figure 5 Radioactive and Simulant CUF Fluxes for the Baseline Precipitation

The use of small batches in the R1 and radioactive tests meant that the precipitate slurry filtered each day had just been precipitated, versus the R2 test where the precipitate slurry at the end was about two days old. Conversely, running the R1 and radioactive tests over several days meant that the precipitate slurry at the end was seven or more days old versus only two days for the R2 test. These precipitate slurries are usually found to agglomerate over time when not subjected to shearing, but since the precipitate slurry was pumped each day in the R1 tests, agglomeration would not seem to be a factor.

Another observation was that the permeate from all of the filtrations had small amounts of a very fine precipitate after standing for about one week even though the permeate was initially transparent (turbidity <5 NTU). For R1 and radioactive tests run over several days, this slow precipitation of very fine particles may have occurred in the slurry, resulting in a harder to filter slurry; for the R2 test over only two days, the amount of precipitation would have been much less. Additional evidence for this slow precipitation comes from the alternate precipitation method tests. In these tests, the permeate produced was somewhat orange, while the baseline

precipitations produced yellowish-green permeate. The alternate precipitation permeates produced fine precipitates like the baseline permeates, but did so much faster. The orange color may have been due to sub-micron particles of precipitate slurry that passed through the filter, but did not result in an increase in measured turbidity. This orange color would seem to be indicative of more fine particles, and indeed, the alternate method precipitates filtered much more poorly that the baseline method precipitates. Also, particle size measurements were made using permeate as the diluent so that precipitation or dissolution of the slurry would be minimized. The alternate precipitation permeate could not be used as the diluent because it had too high an absorbance for the Microtrac analyzer to be zeroed. The analyzer could not quantify any particulate, but the inability to zero it definitely indicates that sub-micron particles may have been present.

The cleanliness of the filter was tested by measuring the clean water flux and the flux with a 5 wt% strontium carbonate slurry. No significant differences were seen between the R1 and R2 tests. However, the R2 concentration test was conducted after an extended period of soaking in nitric acid, so the filter may have been cleaner even though the flux tests were inconclusive.

None of the possible reasons given above account fully for the differences in filtration flux, but taken together they may account for the observed data.

Comparison of Baseline and Alternate Precipitation Fluxes

A comparison of the fluxes for the R2 baseline and alternate precipitation methods are shown in Figure 6 for both the CUF and the pilot unit. The differences between the baseline and alternate precipitation slurries suggest that there is some characteristic of these slurries that is significantly different. As previously discussed, the slow precipitation of fine particles may be a factor, but the physical properties of each precipitate slurry were also examined for differences.

Figure 7 and Figure 8 show the precipitate slurry viscosity and yield stress as a function of the undissolved solids content for each of the tests. All of the slurries were approximately Newtonian before they were concentrated, with insignificant yield stresses. The yield stress of the baseline precipitation slurries increased in a roughly linear manner as the undissolved solids content was increased. As shown in Figure 10, these data are much more scattered than the viscosity data shown in Figure 9. The alternate precipitation method slurry showed a much steeper increase in the yield stress than the baseline precipitate slurry. This increase was similar to the increase seen for the baseline precipitate slurry when it was washed with 0.01M NaOH to remove the soluble species. The washed baseline precipitate slurry filtered no differently than the unwashed precipitate slurry (except for the permeate viscosity effect), so yield stress would not seem to correlate with the filtration flux.

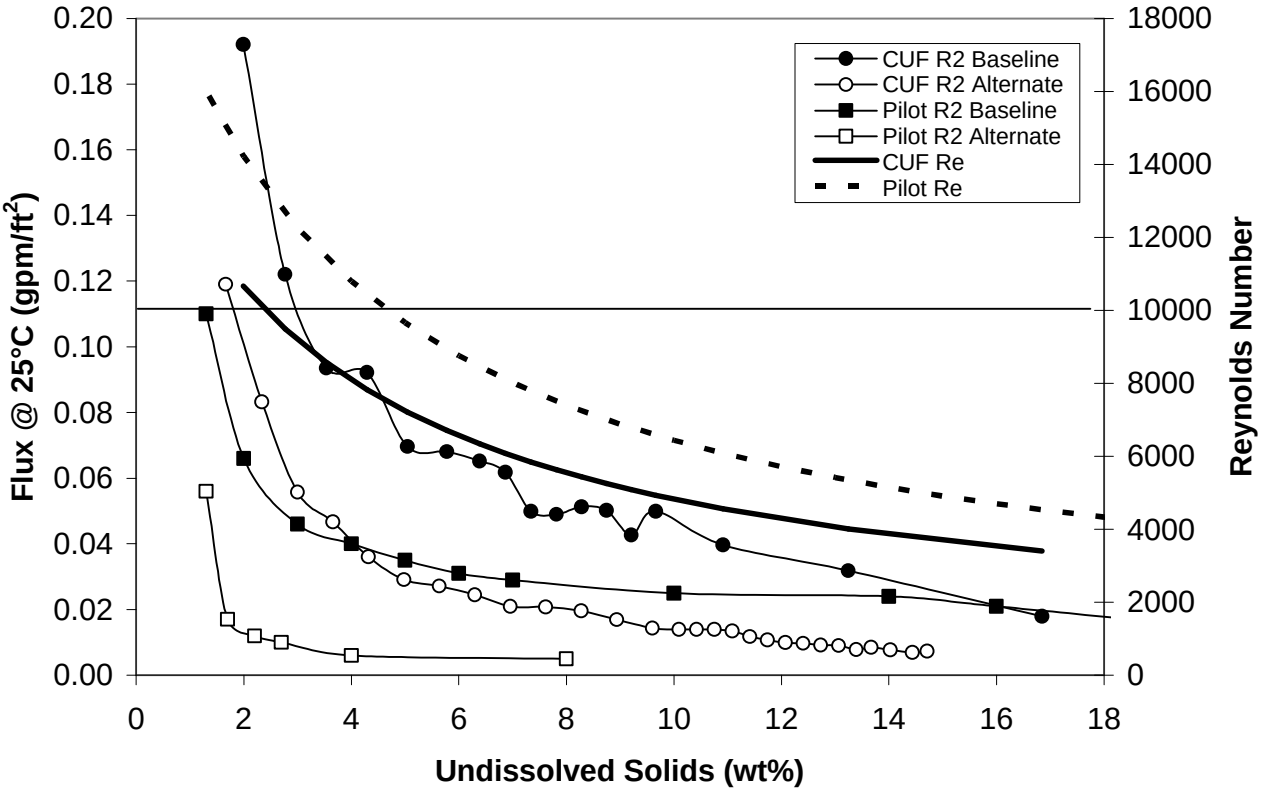

Figure 6 Comparison of Baseline and Alternate Precipitation Fluxes

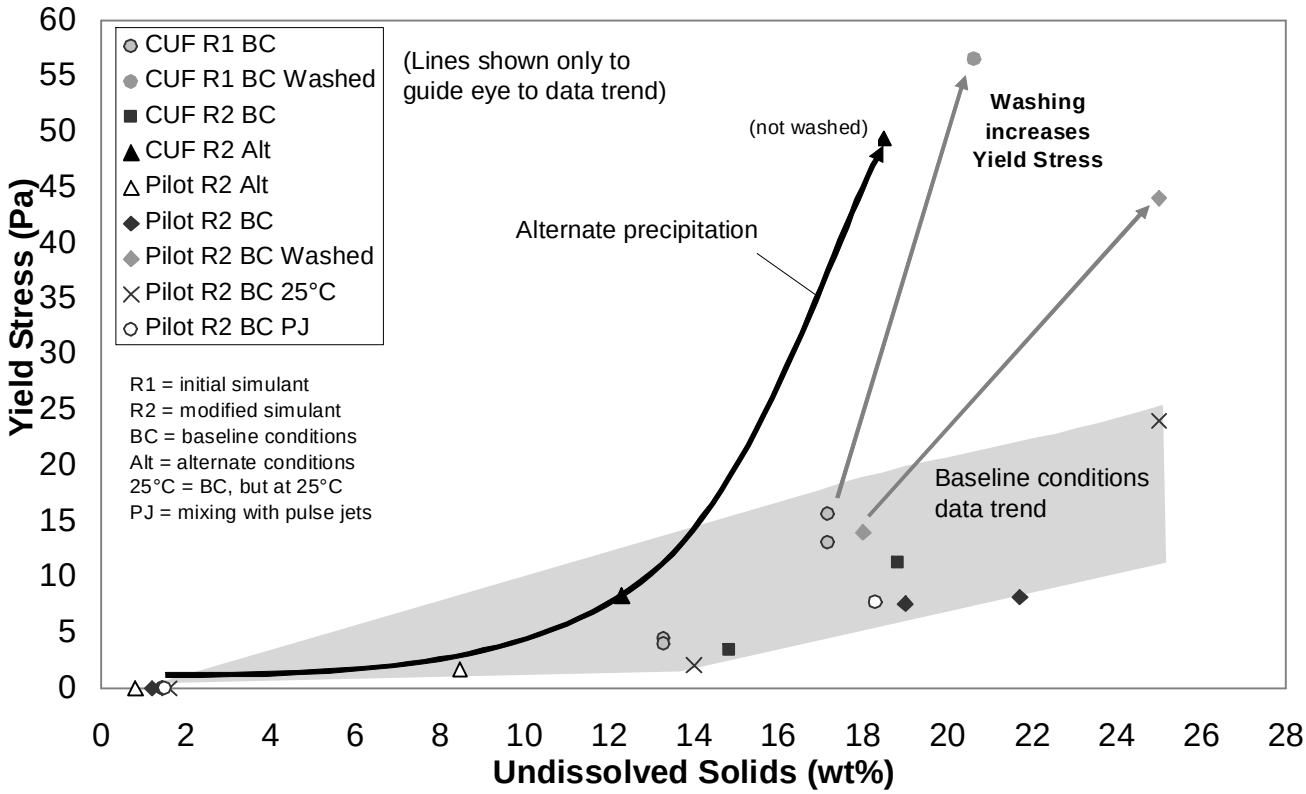

Figure 7 Slurry Yield Stresses

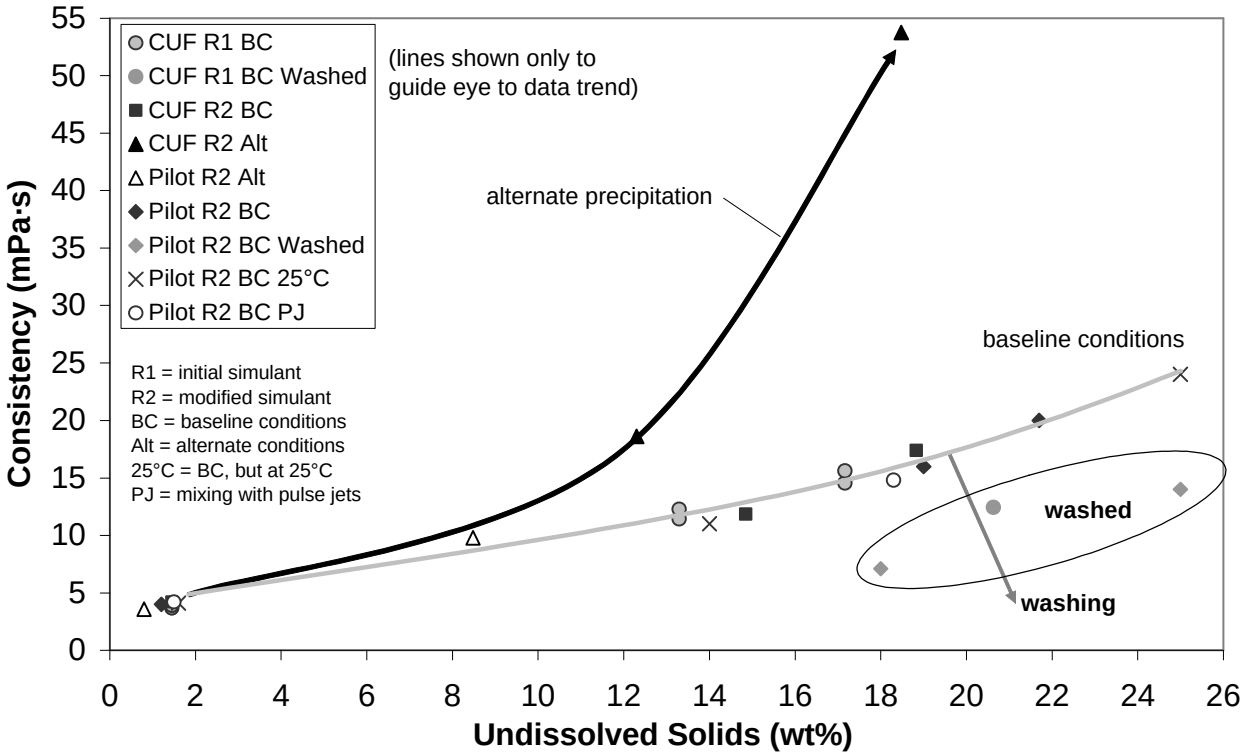

Figure 8 Slurry Viscosity

The viscosity of the baseline precipitates followed an approximately linear trend with respect to the undissolved solids content, but the alternate precipitation method showed a steep increase in viscosity with solids content similar to that found for the yield stress. The viscosity was 54 mPa·s at ~19 wt% versus only 16 mPa·s for the baseline precipitate slurry. Washing of the slurries reduced the dissolved solids content, thus reducing the viscosity due to the decrease in viscosity of the permeate. The viscosity does appear to have an effect on the flux, as shown in Figure 9. The viscosity of the alternate precipitation slurry increases almost exponentially above 8 wt% undissolved solids. The slurry viscosity moving towards the wall would also increase in a similar way, so the viscosity at the wall may be a factor in the observed behavior.

Equation 10 predicts that the filtration flux will depend on the cake viscosity to the -1/3 power, given all other properties to be constant. The cake hydraulic resistivity, among other parameters, is not necessarily the same for the different precipitate slurries. However, the effect of the cake viscosity can still be examined. For two fluids with different cake viscosities, the flux ratio is:

$$\frac{J_2}{J_1} = \left(\frac{m_{C1}}{m_{C2}} \right)^{1/3} \qquad \text{Equation 17}$$

If we assume that the cake viscosity ratio can be approximated by the viscosity ratio at 19 wt% solids, the predicted flux ratio is then $(54/16)^{1/3}$, or 1.5. Figure 9 shows the alternate precipitation data adjusted upward by this factor.

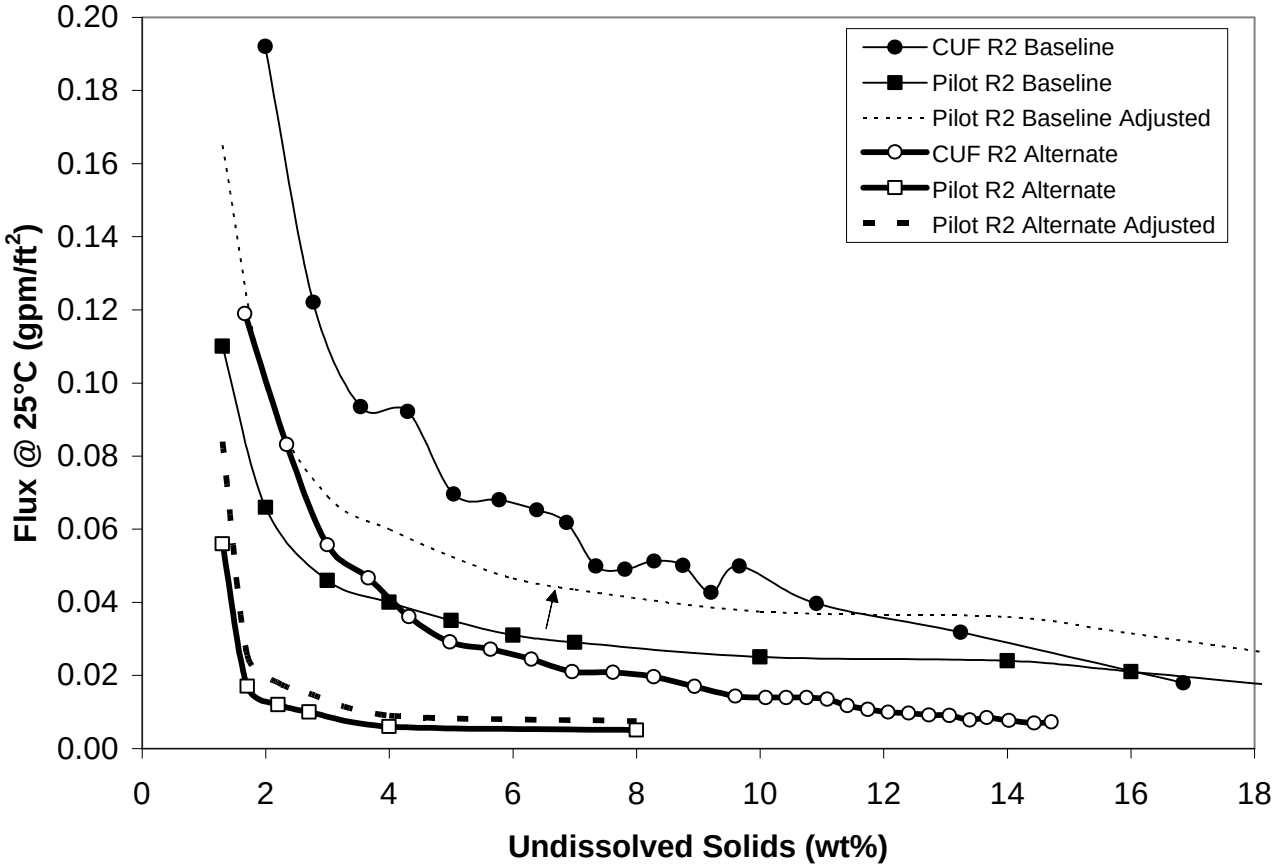

Figure 9 Adjustment of Alternate Precipitation Fluxes for Cake Viscosity

This adjustment makes the different test results closer together, but there are still differences. The steeply increasing viscosity of the alternate precipitate slurry suggests that the ratio may be larger, which would make the correction better.

Figure 10 also shows pilot data for the baseline precipitation conducted at 25°C versus 50°C and with pulse jet mixers used rather than an agitator. Both of these changes resulted in lower filtration fluxes. Lower temperature and pulse jet mixing seem to have effects similar to using the alternate precipitation. The lower precipitation temperature is the same temperature used in the alternate precipitation method, so temperature definitely affects the filterability of the precipitate slurry.

The pulse jet mixing method is much less energetic compared to mechanical agitation, so the degree of agitation is also important. This conclusion is consistent with 50L precipitation tests that were done. Both tests used mechanical agitation, but one test was done in a tank without baffles and the other with baffles and also with faster agitation. The test with baffles and more agitation resulted in a more filterable precipitate slurry.

These differences in precipitation method show that the method has definite effects on the filtration flux that can be achieved. The differences in the flux are actually due to some physical difference or differences in the precipitate slurries, but what these differences are has not been fully determined.

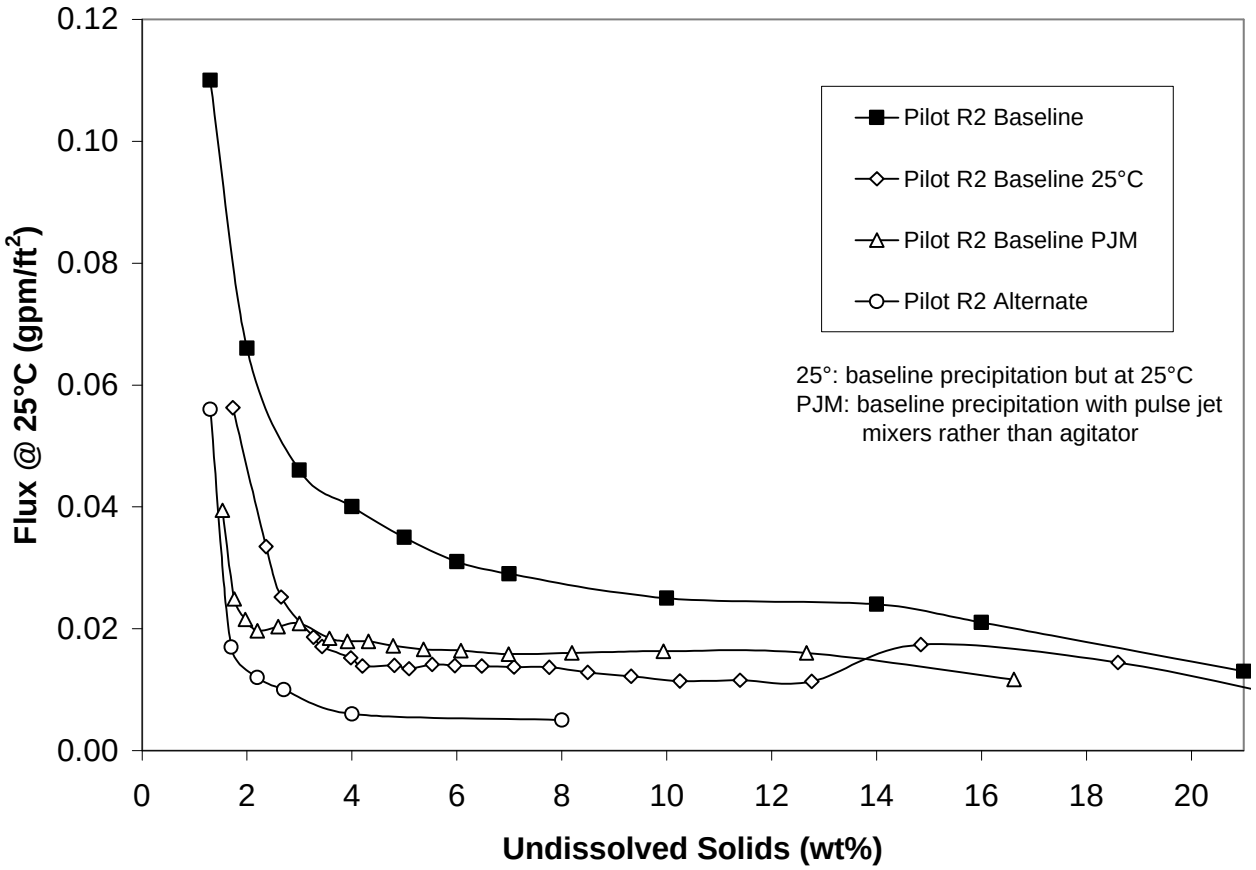

Figure 10 Comparison of Pilot Fluxes

Effects of Filter Size (Scale) on the Filtration Flux

For all the tests performed, the pilot unit results were always lower than the CUF results for the same feed slurry. These differences were shown in Figure 6. Several possible reasons that were postulated are:

- The slurry in the pilot unit is degraded to smaller particle sizes more than in the CUF, resulting in a more difficult to filter slurry.
- The shear stress at the wall for the same axial velocity is higher in the CUF than in the pilot, which would be expected to result in higher fluxes.
- The pilot unit tubes are longer than the CUF tubes. Therefore, a higher percentage of the length of the CUF tubes is subject to entrance effects, which would tend to give higher mass transfer coefficients and fluxes in the CUF.

The first reason was shown earlier to be false. Duignan (Duignan 2003) calculated, using computational fluid dynamics, that the combination of higher shear stress and the entrance effects results in about 30% greater average shear stress in the CUF. The smaller diameter tube in the CUF results in a higher shear stress at the wall and the shorter length means more

the CUF tube will be in the entrance length region where turbulence is greater. The empirically determined dependence of flux on velocity was to about the 0.6 power, which equals a shear stress dependence to about the 1/3 power.

A 30% increase in shear stress would then result in a 9% increase in flux. The actual pilot unit fluxes were 10-60% lower than in the CUF for the baseline precipitate slurry and 75-87% lower for the alternate precipitation slurry, so the shear stress differences do not account for all of the differences. Figure 6 also shows the Reynolds numbers for both the CUF and pilot baseline test data. Most of the data is in the transition region between laminar and fully turbulent flow, where most models for flow and mass transfer are of limited validity. Arbitrarily applying the concentration polarization model for laminar flow gives the flux dependence:

$$\frac{J_P}{J_C} = \frac{D_C^{1/3} L_C^{1/3}}{D_P^{1/3} D_P^{1/3}} \approx 0.91 \times 0.64 = 0.58$$

where C indicates CUF, P indicates pilot

The pilot flux for the baseline precipitation was on average about 47% of the CUF flux, but the alternate precipitation pilot flux was on average only 21% of the CUF flux. To understand the differences in the performance of the pilot filter and the CUF filter, additional data in more controlled experiments would be needed to determine the causes of these differences.

Conclusions

1. The R1 baseline precipitation CUF test validated the simulant since it gave essentially the same flux as the radioactive CUF test.

2. Multiple precipitations with filtration of several days resulted in lower fluxes than a single precipitation with filtration over two days or less.

3. The alternate precipitation method results in more difficult to filter slurries.

4. The volume particle size distribution of filtered slurries for the alternate precipitation has more particles in the 6-11 μm range than the baseline precipitation. This difference appears to be correlated with filterability.

5. Flux data at constant undissolved solids concentration was dependent on velocity and elapsed time (particle degradation). The effect of transmembrane pressure was statistically insignificant. The velocity dependence (~0.6 power) is consistent with the model of Datta (Equation 10, ~0.58 power), and is also close to the concentration polarization model (0.8 power).

6. The flux versus undissolved solids concentration was fit by an equation with a dependence on $\ln \frac{C_W}{C_B}$ and the inverse of permeate viscosity.

7. The viscosity of the alternate precipitation slurries increased significantly with solids concentration compared to a much smaller increase for the baseline precipitation slurries.

8. The model of Datta suggests that the flux should be inversely proportional to the cake viscosity to the 1/3 power, or $\frac{J_2}{J_1} = \left(\frac{m_{C1}}{m_{C2}} \right)^{1/3}$, so the alternate precipitation slurry would be expected to have a lower flux since its estimated cake viscosity was higher.

9. The differences in wall shear stress and entrance effects account for only some of the greater flux in the CUF compared to the pilot unit.

References

Datta, S., Gaddis, J. L. (1997). *Dynamics and Rheology of Fouling Cakes Formed During Ultrafiltration.* Separation Science & Technology **32**(1-4): 327-353.

Duignan, M. R., *Final Report: Pilot-Scale Cross-Flow Ultrafiltration Test Using a Hanford Site Tank 241-AN-102 Waste Simulant*, **USDOE Report WSRC-TR-2003-00204, Rev. 0**, Westinghouse Savannah River Co. (2003).

Eibling, R. E., *Development of a Supernate Simulant for Hanford Tank 241-AN-102 Waste*, **USDOE Report WSRC-TR-2002-00040, Rev. 0**, Westinghouse Savannah River Co. (2002).

Nash, C. A., Rosencrance, S. W., Walker, W. W., Wilmarth, W. R., *Investigation of Varies Strontium-Transuranic Percipitation Chemistries for Crossflow Filtration*, **USDOE Report BNF-003-98-0171, Rev. 0**, Westinghouse Savannah River Co. (2000a).

Nash, C. A., Rosencrance, S. W., Wilmarth, W. R., *Entrained Solids, Strontium-Transuranic Precipitation, and Crossflow Filtration of AN102 Small C*, **USDOE Report WSRC-TR-2000-00341, Rev. 0**, Westinghouse Savannah River Co. (2000b).

Nash, C. A., Saito, H. H., Wilmarth, W. R., *Strontium-Transuranic Precipitation and Crossflow Filtration of 241-AN-102 Large C*, **USDOE Report WSRC-TR-2000-00506, Rev. 0**, Westinghouse Savannah River Co. (2001).

Porter, M. C. (1972). *Concentration Polarization with Membrane Filtration.* Chem. Prod. Res. Develop. **11**(3): 234-238.

Porter, M. C. (1990). Handbook of Industrial Membrane Technology. Park Ridge, NJ, Noyes Publications.

Zamecnik, J. R., Baich, M. R., Hansen, E. K., Poirier, M. R., *AN-102 Simulant Sr/TRU Precipitation and Ultrafiltration*, **USDOE Report WSRC-TR-2003-00056, Rev. 0**, Westinghouse Savannah River Co. (2003).